

# PbIn<sub>6</sub>Te<sub>10</sub>: new nonlinear crystal for three-wave interactions with transmission extending from 1.7 to 25 μm

Samvel Avanesov,<sup>1</sup> Valeriy Badikov,<sup>1</sup> Aleksey Tyazhev,<sup>2</sup> Dmitrii Badikov,<sup>1</sup>  
Vladimir Panyutin,<sup>2</sup> Georgi Marchev,<sup>2</sup> Galina Shevyrdyaeva,<sup>1</sup> Konstantin Mitin,<sup>1</sup>  
Frank Noack,<sup>2</sup> Polina Vinogradova,<sup>1</sup> Nadezhda Schebetova,<sup>1</sup> Valentin Petrov,<sup>2,\*</sup> and  
Albert Kwasniewski<sup>3</sup>

<sup>1</sup>High Technologies Laboratory, Kuban State University, 149 Stavropolskaya Str., 350040 Krasnodar, Russia

<sup>2</sup>Max-Born-Institute for Nonlinear Optics and Ultrafast Spectroscopy, 2A Max-Born-Str., D-12489 Berlin, Germany

<sup>3</sup>Leibniz Institute for Crystal Growth, 2 Max-Born-Str., D-12489 Berlin, Germany

\*petrov@mbi-berlin.de

**Abstract:** We have grown single crystals of PbIn<sub>6</sub>Te<sub>10</sub>, with clear transparency from 3 to 20 μm, and showed that this new nonlinear material possesses sufficient birefringence for phase-matching of three-wave parametric interactions and a nonlinear coefficient of 51 pm/V.

©2011 Optical Society of America

**OCIS codes:** (190.4400) Nonlinear optics, materials; (190.4410) Nonlinear optics, parametric processes.

---

## References and links

1. V. G. Dmitriev, G. G. Gurzadyan, and D. N. Nikogosyan, *Handbook of Nonlinear Optical Crystals*, 3rd revised edition (Springer, 1999).
2. H. Iijima, R. Nagai, N. Nishimori, R. Hajima, and E. J. Minehara, "Frequency-resolved optical gating system with a tellurium crystal for characterizing free-electron lasers in the wavelength range of 10-30 μm," *Rev. Sci. Instrum.* **80**(12), 123106 (2009).
3. J. Xu, G. M. H. Knippels, D. Oepts, and A. F. G. Van der Meer, "A far-infrared broadband (8.5-37 μm) autocorrelator with sub-picosecond time resolution based on cadmium telluride," *Opt. Commun.* **197**(4-6), 379-383 (2001).
4. P. G. Schunemann, S. D. Setzler, T. M. Pollak, M. C. Ohmer, J. T. Goldstein, and D. E. Zelmon, "Crystal growth and properties of AgGaTe<sub>2</sub>," *J. Cryst. Growth* **211**(1-4), 242-246 (2000).
5. L. Isaenko, P. Krinitsin, V. Vedenyapin, A. Yelissev, A. Merkulov, J.-J. Zondy, and V. Petrov, "LiGaTe<sub>2</sub>: a new highly nonlinear chalcopyrite optical crystal for the mid-IR," *Cryst. Growth Des.* **5**(4), 1325-1329 (2005).
6. H. J. Deiseroth and H. D. Müller, "Structural relations in the family of nonmetallic filled β-manganese phases: the new members A<sub>2</sub>Ga<sub>6</sub>Te<sub>10</sub> (A: Sn, Pb) and PbIn<sub>6</sub>Te<sub>10</sub>," *Z. Anorg. Allg. Chem.* **622**(3), 405-410 (1996).
7. L. Kienle and H. J. Deiseroth, "SnAl<sub>6</sub>Te<sub>10</sub>, SnGa<sub>6</sub>Te<sub>10</sub> and PbGa<sub>6</sub>Te<sub>10</sub>: superstructures, symmetry relations and structural chemistry of filled β-manganese phases," *Z. Kristallogr.* **213**(11), 569-574 (1998).
8. V. Petrov, F. Noack, I. Tunchev, P. Schunemann, and K. Zawilski, "The nonlinear coefficient d<sub>36</sub> of CdSiP<sub>2</sub>," *Proc. SPIE* **7197**, 71970M (2009).

---

## 1. Introduction

The objective of the present work was to search for new inorganic nonlinear crystals for three-wave parametric processes in the near- to far-IR (above 15 μm and up to 25-30 μm) spectral range. The long-wave transparency edge of typical selenide compounds is limited by multi-phonon absorption which starts at 14-18 μm and the transmission drops to zero near 19 μm for AgGaSe<sub>2</sub>, 20 μm for GaSe, and 25 μm for CdSe [1]. The commercially available crystal with longest wavelength limit, CdSe, exhibits unfortunately only modest (~18 pm/V) nonlinearity. Elemental Te, known for more than 35 years, is transparent from 3.5 to 36 μm and possesses the highest known nonlinear coefficient for an inorganic material, ~600 pm/V [1]. However, elemental Te, similar to elemental Se, exhibits high linear losses which do not permit real applications apart from some diagnostics (e.g. of ultrashort pulses) in the far-IR [2]. Some binary non-centrosymmetric telluride crystals with optical quality exist, e.g. CdTe and ZnTe,

but they are cubic and their application as nonlinear crystals is also limited to diagnostics utilizing the relatively long coherence length in the far-IR in the absence of birefringent phase-matching [3]. More recently, single crystals of the chalcopyrite type  $\text{AgGaTe}_2$  (analogue of  $\text{AgGaS}_2$  and  $\text{AgGaSe}_2$  with expected transparency limit around  $25\ \mu\text{m}$ ) were grown with sufficiently large sizes and optical quality, however, the birefringence of this material also turned out to be slightly too small for phase-matching [4]. Another chalcopyrite type telluride,  $\text{LiGaTe}_2$  [5], showed sufficient birefringence, but unfortunately, besides the bad chemical surface stability, the peculiar features of such Li-type ternary compounds leading to extended short-wave transmission also result in shorter long-wave transparency limit ( $<15\ \mu\text{m}$  in the case of  $\text{LiGaTe}_2$ ). On the other hand, it should be emphasized that extended short-wave limit is also an attractive property for any IR nonlinear crystal because it enables pumping at near-IR wavelengths for down conversion and is normally associated with better thermo-mechanical properties and damage resistivity.

Recently, we initiated an investigation of another family of ternary tellurides for which in fact only structural properties were known [6,7]. Deiseroth et al. [6] gave an overview of the X-ray data for crystals with the non-metallic  $\beta$ -Mn phase type, including binary tellurides ( $\text{Ga}_7\text{Te}_{10}$ ,  $\text{In}_7\text{Te}_{10}$ ) and three new ternary compounds synthesized by them ( $\text{SnGa}_6\text{Te}_{10}$  and  $\text{PbIn}_6\text{Te}_{10}$ , for which tiny single crystals could be extracted, and  $\text{PbGa}_6\text{Te}_{10}$ , obtained only in polycrystalline form). These compounds crystallize in the non-centrosymmetric point group  $D_3$  (32), space group  $R32$  ( $D_3^7$ ). In binary tellurides,  $\text{Ga}^{2+}$  ( $\text{In}^{2+}$ ) ions fill the divalent metal sub-lattice in a statistical manner. However, it was noted in [7] that weak super-structural reflections are observed in the ternary tellurides which are associated with Sn(Pb) ordering in the divalent metal sub-lattice. This cation ordering reduces the rhomboedric symmetry of the ternary tellurides to the symmetry of the enantiomorphic pairs  $D_3^4 - D_3^6$  ( $P3_121 - P3_221$ ) [7]. The structural similarity of the binary ( $\text{B}_7\text{Te}_{10}$ ) and ternary ( $\text{AB}_6\text{Te}_{10}$ ) compounds might be an important factor for the crystal growth of the latter, especially in cases when the unit cell volumes and melting temperatures are similar. From the data in [6], we obtained  $V(\text{Ga}_7\text{Te}_{10})/V(\text{PbGa}_6\text{Te}_{10})\sim 0.983$  and  $V(\text{In}_7\text{Te}_{10})/V(\text{PbIn}_6\text{Te}_{10})\sim 1.004$ . Such close values are in fact not unexpected since the binary compounds can be regarded as a degenerate form of the ternary ones, in which the sub-lattice of the trivalent and divalent metals is occupied by the same ion. Thus, when crystallizing e.g.  $\text{PbIn}_6\text{Te}_{10}$  from the melt, it is not obvious which of the two ions,  $\text{In}^{2+}$  or  $\text{Pb}^{2+}$ , will occupy the position of the divalent metal. The nominal concentration of In in the melt will be six times higher than that of Pb but the growth scenario will be governed by the relative segregation coefficients of the two ions for the chosen actual concentrations and thermodynamic conditions.

## 2. Growth and transparency of $\text{PbIn}_6\text{Te}_{10}$

In order to estimate the potential of such crystals for nonlinear optics we attempted to grow, for the first time to our knowledge, large size crystals of  $\text{PbIn}_6\text{Te}_{10}$  and  $\text{In}_7\text{Te}_{10}$ . For the synthesis, high purity (5Ns for Pb and Te and 6Ns for In) raw materials were used.

The melting temperatures were estimated from differential thermal analysis (DTA) and they were  $(630 \pm 5)^\circ\text{C}$  for  $\text{PbIn}_6\text{Te}_{10}$  and  $(670 \pm 5)^\circ\text{C}$  for  $\text{In}_7\text{Te}_{10}$ . The single crystals were grown by the Bridgman-Stockbarger technique with a crystallization front velocity of  $6\ \text{mm/day}$  and a temperature gradient in the crystallization zone of  $10\text{-}15^\circ\text{C/cm}$ . Cooling was performed in the regime of switched-off furnace.

Unfortunately it was impossible to grow high quality binary  $\text{In}_7\text{Te}_{10}$ . Therefore, the further efforts were focused on the ternary  $\text{PbIn}_6\text{Te}_{10}$  (PIT). Single PIT crystals of sizes up to few centimetres were obtained from which optical elements and prisms could be cut (Fig. 1). In view of the above mentioned crystallo-chemical similarity between the binary and ternary compounds, the lower parts of the grown boules were used for a charge composition corresponding to stoichiometric  $\text{PbIn}_6\text{Te}_{10}$ .

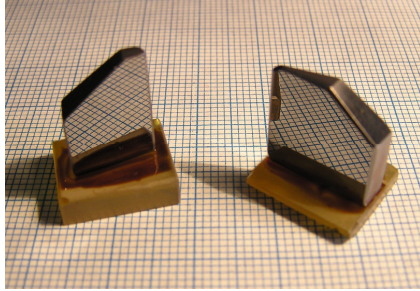


Fig. 1. Prisms of  $\text{PbIn}_6\text{Te}_{10}$  (PIT) prepared for refractive index measurements.

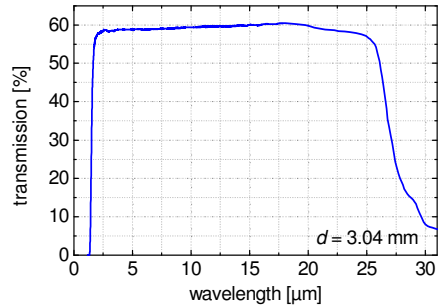


Fig. 2. Unpolarized transmission spectrum of PIT recorded with a ~3 mm thick plate.

The clear transparency of PIT extends from 3 to 20  $\mu\text{m}$  where the absorption coefficient does not exceed  $(0.07 \pm 0.03) \text{ cm}^{-1}$ . At an absorption level of  $0.3 \text{ cm}^{-1}$ , PIT is transparent from 1.7 to 25  $\mu\text{m}$  (Fig. 2), while the zero-level transmission limit (to compare with the given in the introduction values for  $\text{AgGaSe}_2$ ,  $\text{GaSe}$  and  $\text{CdSe}$ ) should be above 31  $\mu\text{m}$ .

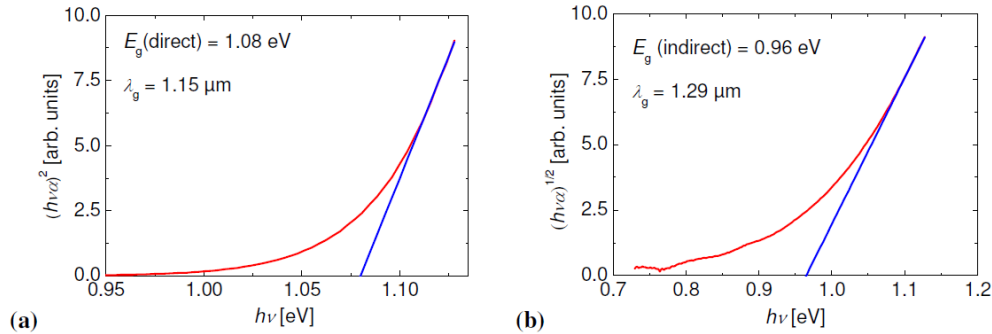


Fig. 3. Direct (a) and indirect (b) band-gap determination of PIT using a 0.25-mm thick plate and unpolarized light.

From the measured absorption coefficient  $\alpha(h\nu)$  and fitting the dependences of  $(h\nu\alpha)^2$  vs  $h\nu$  and  $(h\nu\alpha)^{1/2}$  vs  $h\nu$  we obtained direct and indirect band-gaps of  $E_g(\text{direct}) = 1.08 \text{ eV}$  (1.15  $\mu\text{m}$ ) and  $E_g(\text{indirect}) = 0.96 \text{ eV}$  (1.29  $\mu\text{m}$ ), respectively (Fig. 3).

### 3. Birefringence and nonlinearity

The refractive indices of PIT were measured in the 1.5-10.4  $\mu\text{m}$  spectral range by the auto-collimation method using prisms with an apex angle of about  $12^\circ$  and aperture of  $12 \times 15 \text{ mm}^2$  (Fig. 1). The accuracy was better than 0.005. We found that PIT is optically positive with a characteristic birefringence of  $n_e - n_o \sim 0.05$  which means that it is phase-matchable. From the Sellmeier equations constructed on the basis of the dispersion data measured (Table 1), we

estimated a short-wave second-harmonic generation (SHG) limit of  $\sim 3.6 \mu\text{m}$  (fundamental wavelength). The short- and long-wave SHG limits for ee-o type-I interaction are determined from the solutions of the equation  $\Delta n(\lambda_F) = \delta n(\lambda_F, \lambda_F/2)$ , where  $\Delta n = n_e(\lambda_F) - n_o(\lambda_F)$  is the birefringence at the fundamental and  $\delta n = n_o(\lambda_F/2) - n_o(\lambda_F)$  is a measure for the dispersion of the ordinary wave between the fundamental and the second harmonic. Thus, the long-wave limit can be estimated only from extrapolation of the available refractive index data and it should be around  $21 \mu\text{m}$ . In these two limits, the phase-matching angle approaches  $90^\circ$  and in between it reaches a minimum value of  $32^\circ$  for SHG at  $8.3 \mu\text{m}$  (fundamental).

**Table 1. Sellmeier Coefficients of PbIn6Te10 at Room Temperature:**  
 $n^2 = A_1 + A_3/(\lambda^2 - A_2) + A_5/(\lambda^2 - A_4)$ , Where  $\lambda$  Is in  $\mu\text{m}$

crystal	$n$	$A_1$	$A_2$	$A_3$	$A_4$	$A_5$
PIT 1.5-10.4 $\mu\text{m}$	$n_o$	11.162067	0.720740	0.900821	3153.47	6347.934
	$n_e$	11.938574	0.442087	1.227212	3819.91	9616.588

In optically positive crystals of the  $D_3$  (32) point group the effective nonlinearity for three-wave interactions is given by  $d_{\text{eff}}(\text{oe-o}) = d_{11}\cos\theta\cos 3\varphi$  and  $d_{\text{eff}}(\text{ee-o}) = d_{11}\cos^2\theta\sin 3\varphi$ . The polar and azimuthal angles  $\theta$  and  $\varphi$  are defined in a crystallo-physical frame XYZ (coinciding with the dielectric frame xyz) whose Z axis is parallel to the  $c$ -crystallographic axis (optical axis) and whose X axis is parallel to one of the crystallographic  $a$ -axes.

The nonlinear coefficient  $d_{11}$  of PIT was measured by comparing the SHG efficiency to that obtained with ZnGeP<sub>2</sub> (ZGP). The fundamental beam at  $4.7 \mu\text{m}$  that we used was produced by a femtosecond optical parametric amplifier (OPA) pumped near  $800 \text{ nm}$  at a repetition rate of  $1 \text{ kHz}$ . The OPA used a  $6\text{-mm}$ -long KNbO<sub>3</sub> crystal cut at  $\theta = 41.9^\circ$  for type-I phase-matching. As an OPA seed we used the frequency doubled to  $\sim 1 \mu\text{m}$  idler output of a  $\beta$ -BaB<sub>2</sub>O<sub>4</sub> (BBO) type-II OPA pumped by the same  $800 \text{ nm}$  pump source. The idler pulses of the KNbO<sub>3</sub> OPA at  $4.7 \mu\text{m}$  were temporally broadened but simultaneously spectrally narrowed. More details on this set-up can be found elsewhere [8]. Care was taken to have sufficient spectral and angular acceptance so that these effects and the spatial walk-off due to birefringence could be neglected.

The  $0.48 \text{ mm}$  thick PIT test plate and the  $0.53\text{-thick}$  ZGP reference sample were cut at  $\theta = 48^\circ$ ,  $\varphi = 30^\circ$ , and  $\theta = 50.5^\circ$ ,  $\varphi = 0^\circ$ , respectively. The angular acceptance (FWHM) amounts to  $5.8^\circ$  for PIT and  $5^\circ$  for ZGP and the birefringence angle is  $\rho = 0.9^\circ$  in PIT and  $\rho = 0.7^\circ$  in ZGP. The group velocity mismatch amounts to  $170 \text{ fs/mm}$  for PIT and  $70 \text{ fs/mm}$  for ZGP, this difference could only lead to underestimation of the PIT nonlinearity but with  $350 \text{ fs}$  long fundamental pulses at  $4.7 \mu\text{m}$  (typical spectral FWHM of  $100 \text{ nm}$ ) it is not expected to cause significant error. For a fundamental energy of  $3\text{-}4 \mu\text{J}$ , the spot size was selected large enough so that spatial walk-off effect was negligible and the internal energy conversion efficiency remained below  $10\%$  (small signal approximation). The observed phase-matching angles for both samples were very close to the cut angles and for calculation of the relative nonlinearities we only took into account the effect of the different index of refraction on the Fresnel losses and the coupling coefficient.

For both crystals we performed 5 test series, each of them consisting of 8-10 measurements with fine crystal tuning on a SHG signal maximum. The results can be summarized as:  $d_{\text{eff}}(\text{PIT}) = (0.290 \pm 0.015) \cdot d_{36}(\text{ZGP})$  or  $d_{11}(\text{PIT}) = (0.647 \pm 0.034) \cdot d_{36}(\text{ZGP})$ . Having in mind that  $d_{36}(\text{ZGP}) = 79 \text{ pm/V}$  for this process [8], we arrived at  $d_{11}(\text{PIT}) = (51 \pm 3) \text{ pm/V}$ .

#### 4. Homogeneity

As already mentioned, PbIn<sub>6</sub>Te<sub>10</sub> and In<sub>7</sub>Te<sub>10</sub> have similar composition, structure, and melting points while the unit cell volume differs by less than  $0.5\%$ . The similarity of all these characteristics implies also similarity in the optical properties of the binary and ternary indium tellurides. As a consequence, it can be expected that the optical properties of the ternary

indium telluride will be rather independent of possible variation of the  $\text{Pb}^{2+}$  content along the height of the boule grown. Unfortunately, it was technically impossible for us to control the composition of the grown crystals neither in radial nor along the growth direction. Nevertheless, we did observe substantial variation of the optical characteristics of the grown crystals along the growth direction of the boule. Such variation in optical properties of crystals grown by the Bridgman-Stockbarger technique is characteristic for solid solutions and is associated with variation of the composition along the growth direction.

In order to investigate the variation of the optical properties of PIT along the growth direction a special boule was grown using an oriented seed. The growth direction was chosen along the normal to the (330) plane defined in the crystallographic frame. From this oriented boule it was possible to fabricate a plate for measurement of the transmission and SHG phase-matching angle dependences on the boule height. The grown boule had a cylindrical shape with a hemispherical “cap” and a conical “nose” in the bottom part. The axis of the cylinder was normal to the crystallo-physical Z-axis (optical axis). After removal of the “cap” and the conical “nose” part (about 10 mm long), the length of the remaining boule amounted to 57 mm. The height  $h$ , used as a parameter, was measured along the growth direction from the bottom, after the removal of the conical part. It should be noted that in the Bridgman-Stockbarger technique crystallization starts with the conical part and ends with the “cap”.

The element prepared for measuring the transmission of the boule was 20.8 mm thick with normal which was parallel to the optical axis. It enabled measurement of the transmission near the short-wave absorption edge for the ordinary polarization along the entire boule height. The absorption level of  $1 \text{ cm}^{-1}$  turned out to be convenient for the given thickness and we measured it with steps of 5 to 7 mm. The wavelength for which this level of absorption is reached is shown in Fig. 4(a) in dependence on the boule height  $h$  (distance from the bottom).

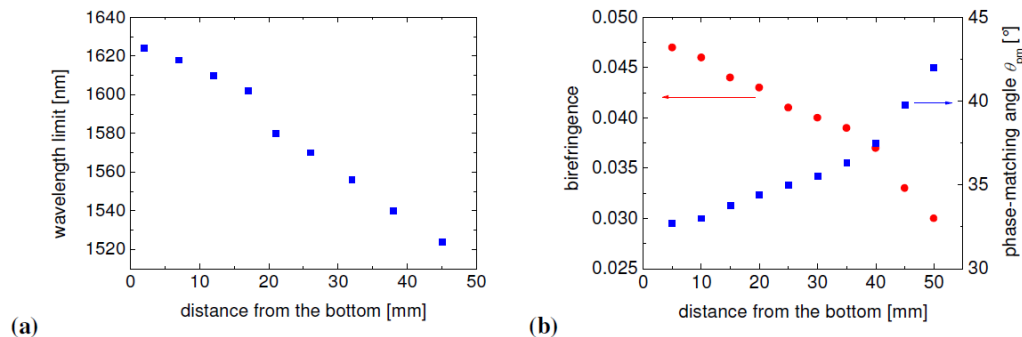


Fig. 4. Dependence of the absorption edge defined at a level of a  $1 \text{ cm}^{-1}$  on the distance from the boule bottom (a) and dependence of the birefringence at  $10.6 \mu\text{m}$  (red circles) and the phase-matching angle for ee-o type SHG at  $10.6 \mu\text{m}$  (blue squares) on the distance from the boule bottom (b).

From the remaining parts of the same boule we fabricated two prisms for measurement of the refractive indices. One of them corresponded to a height of  $h = 10\text{-}15 \text{ mm}$  and the other to a height of  $h = 47\text{-}52 \text{ mm}$ . In both cases the aperture did not exceed  $1 \text{ cm}^2$ . Since for both prisms the refractive angles were far from optimum, the measurements were limited to the spectral range from 1600 to 2000 nm. The results of these measurements were more or less qualitative and will not be tabulated here. The most essential observation seems that near 2000 nm, within the measurement error, the ordinary index of refraction has the same value ( $n_o = 3.070 \pm 0.005$ ) in the upper and lower parts of the boule. It should be noted that the same value for the ordinary index of refraction can be calculated at this wavelength with the Sellmeier coefficients presented in Table 1 which were based on measurements with a different boule (bottom part). Thus, it might be concluded that the index of refraction for the ordinary wave is only weakly dependent on the height. However, the index of refraction for

the extraordinary wave shows a different behavior. In the indicated above spectral range  $n_e(\text{bottom}) - n_e(\text{top}) = 0.025$ . This variation is quite large having in mind that the birefringence in the bottom part amounts to  $\Delta n(\text{bottom}) = 0.05$ . It should be noted that the value of the extraordinary index of refraction in the bottom part,  $n_e(\text{bottom})$ , was 3.120 near 2000 nm, which is rather close to the value of 3.125 that can be calculated from Table 1 for the bottom part from a different boule.

The same plate used for the transmission measurements was then utilized to study the dependence of the SHG phase-matching angle dependence on the height. The type ee - o SHG process was excited with a pulsed (100 ns, 25 mJ) CO<sub>2</sub>-laser operating at 10.6  $\mu\text{m}$  with a repetition rate of 1-2 Hz. Both surfaces were repolished to achieve a different orientation corresponding to a propagation direction defined by  $\theta = 37.3^\circ$  and  $\varphi = 30^\circ$  in the crystallo-physical frame. The final thickness was 16.5 mm while the length of the edge parallel to the growth direction amounted to 55 mm. The beam diameter on the sample was 1.5 mm, measured at a level of  $1/e^2$ . The plate was scanned along the height with a step of 5 mm, measuring at each step the external angle  $\theta_{\text{ext}}$  for maximum SHG signal defined as the angle between the incident beam and the plate normal, with an accuracy of  $0.1^\circ$ . The phase-matching angle  $\theta_{\text{pm}}$  was calculated from  $\theta_{\text{pm}} = \theta_{\text{int}} + \theta$ , using  $\sin \theta_{\text{ext}} = n_e(\theta_{\text{int}} + \theta) \sin \theta_{\text{int}}$ . Since the refractive indices  $n_o$  and  $n_e$  and their dependence on the height were unknown at 10.6  $\mu\text{m}$ , approximate values calculated with the Sellmeier equations from Table 1 were used. The error in the determination of  $\theta_{\text{pm}}$  from this assumption was estimated to be less than  $0.05^\circ$ . The results are shown in Fig. 4(b) together with the birefringence  $\Delta n = n_e(\lambda_F) - n_o(\lambda_F)$  at  $\lambda_F = 10.6 \mu\text{m}$  which was calculated from the phase-matching angles using  $n_o(\lambda_F/2) = n_e(\lambda_F, \theta_{\text{pm}})$  and assuming that  $n_o(\lambda_F/2)$  and  $n_o(\lambda_F)$  are constant along the boule height. It can be seen that both the birefringence and the phase-matching angle show weaker dependence on the height in the bottom part of the boule.

## 5. Conclusion

In conclusion, we grew for the first time to our knowledge nonlinear crystals of PbIn<sub>6</sub>Te<sub>10</sub>, with good transparency extending from the near-IR to above 25  $\mu\text{m}$  and showed that this crystal possesses sufficient birefringence for phase-matching. Its quite high nonlinear coefficient of 51 pm/V, combined with such a wide transparency, could make it a unique material for nonlinear frequency conversion in the mid- and far-IR spectral ranges. It could be pumped by Er<sup>3+</sup>-laser sources operating in the 2.9  $\mu\text{m}$  spectral range, Cr<sup>2+</sup>-lasers in the 2.5  $\mu\text{m}$  spectral range (still without substantial two-photon absorption) or even, after improvement of the residual loss, near 2- $\mu\text{m}$ , by well established powerful Ho<sup>3+</sup>- or Tm<sup>3+</sup>-laser based systems.

## Acknowledgments

The research leading to these results has received funding from the European Community's Seventh Framework Programme FP7/2007-2011 under grant agreement n°224042.